Ordering of cross sections for electron capture from He-like targets by fast projectiles

G. W. Shirtcliffe and K. E. Banyard
Department of Physics, University of Leicester, Leicester, England
(Received 11 June 1979)

The continuum-distorted-wave (CDW) method is used to determine total electron-capture cross sections $Q = \Sigma_{nl}\sigma[nl]$ for proton and α-particle projectiles incident on Li^+ in energy ranges of $100 \leq E \leq 3000$ keV and $100 \leq E \leq 10000$ keV, respectively. A configuration-interaction (CI) wave function is used to describe the Li^+ electrons; for comparison, capture cross sections for H^- and He are examined. For each system the percentage change in Q, Δ(HF→CI), is given for progression from a Hartree-Fock (HF) to a CI description of the target electrons. The main emphasis in this work is devoted to a rationalization of the trends observed in the ordering of Q for these three targets. This was achieved by an analysis of the CDW expression for an individual capture cross section $\sigma[nl, n'l']$, where nl and $n'l'$ are the states of the "active" (captured) and "passive" electrons, respectively.

I. INTRODUCTION

For a helium target the cross sections for electron capture by fast protons are adequately described by the continuum-distorted-wave (CDW) method (see, for example, Salin[1] and Belkić and Gayet[2]). Banyard and Szuster[3] examined the sensitivity of such cross sections with respect to improvements in the He wave function up to and beyond the Hartree-Fock (HF) description; a similar study was made by Moore and Banyard[4] for H^-. The CDW method is used here to evaluate the total cross sections $Q = \sum_{nl}\sigma[nl]$ for the following reactions:

$$H^+ + Li^+(1s^2) \rightarrow H\left(\sum nl\right) + Li^{2+}(1s), \quad (1)$$

$$He^{2+} + Li^+(1s^2) \rightarrow He^+\left(\sum nl\right) + Li^{2+}(1s) \quad (2)$$

in the energy ranges 100–3000 and 100–10 000 keV, respectively. For each reaction we calculated the cross sections $\sigma[nl]$ for the capture states $nl \equiv 1s$, $2s$, and $2p$, and Q was then determined by using the n^{-3} rule (see, for example, Salin[1]). Besides examining, in brief, the sensitivity of Q with respect to changes in the $Li^+(1s^2)$ wave function, we also analyze the CDW expression for a general capture cross section $\sigma[nl, n'l']$, where nl and $n'l'$ are the states of the "active" (captured) and "passive" electrons, respectively, in order to rationalize the trends observed when comparing the cross sections for capture from H^-, He, and Li^+.

II. RESULTS AND DISCUSSION

The capture cross section $\sigma[nl]$ for a given projectile energy E may be written as

$$\sigma[nl] = 2\int_0^\infty b\,|a_{nl}(b)|^2 db$$

(in units of πa_0^2, with a_0 as the atomic unit of length), where $a_{nl}(b)$ is the prior form of the CDW transition amplitude and b is the impact parameter. In Table I we report the total cross sections Q for reactions (1) and (2), and for comparison we tabulate the corresponding results for He and H^-; in each case the target electrons are described by the 35-term configuration-interaction (CI) wave function of Weiss.[5] To assess the influence of electron correlation we also quote for each energy E the percentage change Δ(HF→CI) in Q when going from the HF to the CI description of the target electrons. The HF wave functions for He and Li^+ were those of Clementi and Roetti,[6] and for H^- the fitted functions of Curl and Coulson[7] were used. The Δ(HF→CI) values are seen to reflect a rapid decrease in the importance of correlation as we progress from H^- to Li^+. For a given target it was noted that at a common projectile velocity the proton and α-particle reactions possessed similar Δ(HF→CI) values, the magnitude being almost identical at *high* velocities.

When $E > 100$ keV, Table I shows that the ordering in Q for each projectile is $Q(Li^+) > Q(He) > Q(H^-)$. As E becomes larger the difference between the cross sections for the three systems increases; for example, for protons at 200 keV, $Q(Li^+) \simeq 9Q(H^-)$, whereas at 3000 keV we have $Q(Li^+) \simeq 150Q(H^-)$.

In attempting to account for the above ordering in Q, we note first that the three systems differ in the size of the distortion acting on the captured, or active, electron in the exit channel. Since in the present form of the CDW method the distortion is a function of the net charge on the residual target (see Belkić and Janev[8]) and thus opposes electron capture, its effect should be to produce an ordering of Q which is the reverse of that observed. Second, although the energy de-

TABLE I. Total electron-capture cross sections Q, in units of πa_0^2, for targets H^-, He, and Li^+ for both proton and α-particle projectiles. Each system is described by the 35-term configuration-interaction (CI) function of Weiss,[5] and in square brackets we give the percentage change [Δ(HF → CI)] in going from the Hartree-Fock (HF) to the CI description for the target electrons; Δ(HF → CI) is defined as $[(Q_{CI}-Q_{HF})/Q_{HF}]\times 100\%$.

	Protons				α particles		
E (keV)	H^- [Δ(HF → CI)]	He[a] [Δ(HF → CI)]	Li^+[b] [Δ(HF → CI)]	E (keV)	H^- [Δ(HF → CI)]	He[a] [Δ(HF → CI)]	Li^+[b] [Δ(HF → CI)]
100	6.681^{-2}[c] [−19.8%]	3.482^{-1} [−4.0%]	1.394^{-1} [−4.5%]	100	1.630^{+1} [−16.4%]	5.196^{+1} [−4.7%]	4.695^{+1} [−5.8%]
200	3.922^{-3} [−17.1%]	3.477^{-2} [−3.8%]	3.683^{-2} [−2.2%]	500	1.700^{-1} [−16.9%]	1.512^{0} [−3.8%]	2.084^{0} [−1.9%]
500	5.585^{-5} [−15.9%]	8.456^{-4} [−4.2%]	2.118^{-3} [−1.3%]	1 000	1.268^{-2} [−16.6%]	1.661^{-1} [−4.1%]	3.446^{-1} [−1.4%]
800	5.200^{-6} [−15.9%]	9.912^{-5} [−4.3%]	3.275^{-4} [−1.4%]	2 000	6.619^{-4} [−16.4%]	1.203^{-2} [−4.1%]	3.624^{-2} [−1.3%]
1000	1.622^{-6} [−16.0%]	3.418^{-5} [−4.3%]	1.254^{-4} [−1.4%]	4 000	2.460^{-5} [−16.0%]	5.947^{-4} [−4.4%]	2.396^{-3} [−1.5%]
2000	3.864^{-8} [−16.2%]	1.064^{-6} [−4.4%]	4.995^{-6} [−1.6%]	6 000	3.138^{-6} [−16.1%]	8.794^{-5} [−4.5%]	4.052^{-4} [−1.6%]
3000	4.083^{-9} [−16.3%]	1.270^{-7} [−4.4%]	6.633^{-7} [−1.7%]	10 000	2.104^{-7} [−16.3%]	6.932^{-6} [−4.5%]	3.664^{-5} [−1.7%]

[a] The results for He supersede those reported by Banyard and Szuster (Ref. 3), which contained a small computing error.

[b] Total capture cross section Q was obtained from the "Oppenheimer n^{-3} rule": $Q\simeq\sigma[1s]+1.616(\sigma[2s]+\sigma[2p])$.

[c] Superscript denotes the power of 10 by which each entry should be multiplied.

crement $\Delta\epsilon$ (defined as the difference in energy between the initial and final atomic states and determined here from the theoretical values) is different for each of the three systems, the cross sections are found to become insensitive to $\Delta\epsilon$ in the limit of high projectile velocities. Therefore it would appear that the observed trends in Q must be dominated by the differences in the target wave functions.

We now proceed by analysis of the individual CDW cross section $\sigma[nl,n'l']$ to account for the trends in Q for the more general reaction

$$Z_A+(Z_B,e_1,e_2)\rightarrow(Z_A,e_1)_{nl}+(Z_B,e_2)_{n'l'} \qquad (3)$$

when the target electrons are described by an HF wave function

$$\Phi(1,2)=\sum_p c_p\varphi_p(1)\sum_q c_q\varphi_q(2)\,,$$

where each member of the basis set $\{\varphi\}$ is normalized and the coefficients c_p and c_q are the usual variation constants. The CDW cross section $\sigma[nl,n'l']$ for a relative impact velocity v corresponding to an energy E, when the capture state wave function is $\Psi_{nl}(1)$, can be expressed as

$$\sigma[nl,n'l']=N\left[I\left(\sum_q c_q\varphi_q(2)\,\middle|\,n'l'\right)\right]^2\int_0^\infty\left|\sum_p c_p f_1(\eta,v,\varphi_p(1),\Delta\epsilon)g_1(\eta,v,\varphi_p(1),\Psi_{nl}(1),\nu_1,\nu_2,\Delta\epsilon)\right|^2 d\eta\,, \qquad (4)$$

where N is a constant and $I(\sum_q c_q\varphi_q(2)\,|\,n'l')$ is an overlap integral between the initial and final states which describe the passive electron e_2. The integration over η is a result of performing a Fourier transform of the transition amplitude from position space to a two-dimensional vector space $\vec{\eta}$ (see Belkić and Janev[6]), and the functions ν_1 and ν_2 arise from the distortions due to Coulomb interactions acting in the entrance and exit channels, respectively, and are defined as $\nu_1=Z_A/v$ and $\nu_2=(Z_B-1)/v$. We note that f_1 and g_1 are both functions of $\varphi_p(1)$, and hence the strong dependence of the ordering in the cross sections on $\Phi(1,2)$ is still not apparent. However, since

the occurrence of the distortion in the exit channel *inhibits* capture, we can, without prejudice, proceed with our analysis by setting $\nu_2 = 0$ for the general reaction (3). As a consequence of this, the $\varphi_p(1)$ dependence in g_1 is now removed and the expression for $\sigma[nl, n'l']$ when $\nu_2 = 0$ becomes

$$\sigma[nl, n'l']_{\nu_2=0} = NI^2 \int_0^\infty \left[F_1\left(\eta, v, \sum_p c_p \varphi_p(1), \Delta\epsilon\right)\right]^2 \times |G_1(\eta, v, \Psi_{nl}, \nu_1, \Delta\epsilon)|^2 d\eta . \quad (5)$$

Except for the presence of the energy decrement $\Delta\epsilon$, the functional form of G_1 is independent of the target parameters. At high projectile velocities, G_1 is found to be insensitive to $\Delta\epsilon$, and thus for a particular capture state (nl) the function G_1 becomes identical for our three examples of a two-electron target (Z_B, e_1, e_2). When the basis set $\{\varphi\}$ is represented, for example, by Slater-type orbitals (STO's), the function F_1 takes the form

$$F_1 = \sum_p c_p (-1)^{s_p} N(s_p, \xi_p) \times \frac{\partial^{(s_p-1)}}{\partial \xi_p^{(s_p-1)}} \left(\frac{\xi_p}{[\xi_p^2 + \eta^2 + (v/2 + \Delta\epsilon/v)^2]^2} \right), \quad (6)$$

where s_p, ξ_p, and $N(s_p, \xi_p)$ are the principal quantum number, orbital exponent, and normalization constant, respectively, of the basis function φ_p. Analysis of F_1^2 shows that it represents the probability density of finding the active electron e_1 with a z component of momentum equal to $|v/2 + \Delta\epsilon/v|$ or, conversely, of finding e_1 with a total momentum $p \geq |v/2 + \Delta\epsilon/v|$, and therefore F_1^2 can be interpreted as a two-dimensional momentum density. We note that the z component of momentum is not unique, and its definition is simply a consequence of choosing our coordinate system such that $\vec{\eta} \cdot \vec{v} = 0$, with $\vec{v} \equiv (0, 0, v_z)$.

Let us now particularize reaction (3) by choosing Z_A to be a proton and by setting $nl = n'l' = 1s$ for the targets H^-, He, and Li^+. In Fig. 1 for each system we plot F_1^2 and G_1^2 as a function of η for $\sigma[1s, 1s]_{\nu_2=0}$ at $E = 500$, 1000, and 2000 keV. For subsequent discussion and ease of comparison Table II contains $\sigma[1s, 1s]$ and $\sigma[1s, 1s]_{\nu_2=0}$ at a few selected E; R (as defined later) is a ratio of the cross sections for different targets when $\nu_2 = 0$. Throughout Fig. 1 and Table II each target was described by the HF wave function; for H^- we note that $\sigma[1s, 1s] = [1s, 1s]_{\nu_2=0}$. As anticipated, Fig. 1 shows that the G_1^2 functions for each target are very similar, particularly at large E values. Therefore the ordering of the cross sections in Table II is a direct consequence of the differences in the electron densities in momentum space as represented by F_1^2. When the projectile velocity is increased, the active electron is captured from regions of increasingly higher momentum within the target atom; thus the cross sections reflect the characteristics of the target wave functions near the origin. Indeed, in the limit as $v \to \infty$ the function F_1 may be expressed as

$$F_1 \xrightarrow[(v \to \infty)]{} \sum_p c_p \left. \frac{\partial \varphi_p(1)}{\partial x_1} \right|_{x_1=0} \frac{1}{(\eta^2 + \frac{1}{4}v^2)^2}, \quad (7)$$

and hence

$$\sigma[nl, n'l']_{\nu_2=0\,(v\to\infty)} \to NI^2 \left(\sum_p c_p \left. \frac{\partial \varphi_p(1)}{\partial x_1} \right)^2_{x_1=0} \times \int_0^\infty |G_2(\eta, v, \Psi_{nl}, \nu_1)|^2 d\eta , \quad (8)$$

where $\vec{x}_1$ is the position vector of the active electron with respect to the target nucleus. The η and v dependence in Eq. (8) occurs only in the new function G_2, and in the limit we note that this

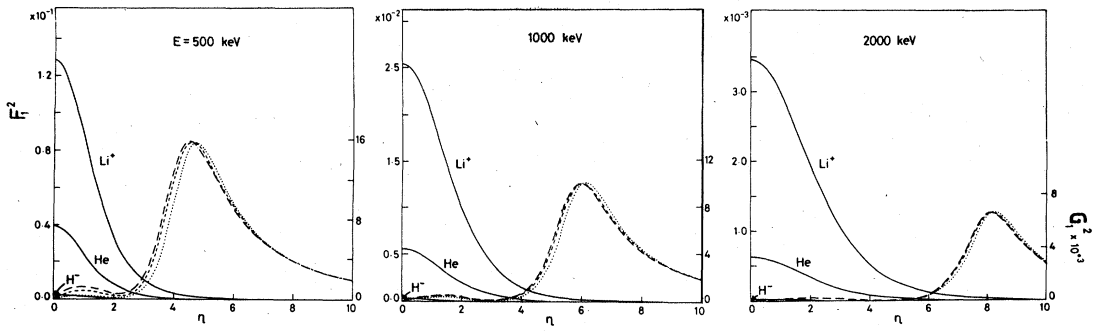

FIG. 1. Plots at three selected impact energies E of F_1^2 and G_1^2 against η for each of the targets H^-, He, and Li^+ corresponding to $\sigma[1s, 1s]_{\nu_2=0}$ in Eq. (5). The projectiles are protons and the target electrons are described by the Hartree-Fock wave functions stated in text. Curves for G_1^2 are long-dashed H^-, short-dashed He, and dotted Li^+.

TABLE II. Cross sections $\sigma[1s,1s]$ and $\sigma[1s,1s]_{\nu_2=0}$, in units of πa_0^2, at selected E for electron capture by protons from the targets H^-, He, and Li^+. Since the distortion in the exit channel due to the Coulomb interaction is zero for H^- (i.e., $\nu_2=0$), we note that $\sigma[1s,1s] = \sigma[1s,1s]_{\nu_2=0}$. We also tabulate values of $R=(\sigma_a[1s,1s]/\sigma_b[1s,1s])_{\nu_2=0}$ for (i) $a\equiv$ He and $b\equiv H^-$ and (ii) $a\equiv Li^+$ and $b\equiv$ He. In each instance the target electrons are described by Hartree-Fock wave functions.

E (keV)	H^-	He	Li^+	He ($\nu_2=0$)	$R_{(i)}$	Li^+ ($\nu_2=0$)	$R_{(ii)}$
500	4.760^{-5} [a]	6.880^{-4}	1.718^{-3}	8.239^{-4}	17.3	1.986^{-3}	2.4
1 000	1.427^{-6}	2.833^{-5}	1.025^{-4}	3.621^{-5}	25.4	1.382^{-4}	3.8
3 000	3.665^{-9}	1.068^{-7}	5.484^{-7}	1.420^{-7}	38.7	8.465^{-7}	6.0
5 000	2.077^{-10}	6.766^{-9}	3.880^{-8}	9.063^{-9}	43.6	6.137^{-8}	6.8
10 000	4.042^{-12}	1.434^{-10}	9.181^{-10}	1.944^{-10}	48.1	1.483^{-9}	7.6

[a] Superscript denotes the power of 10 by which each entry should be multiplied.

function is also independent of $\Delta\epsilon$. Therefore, if we examine the ratio $R[nl,n'l']$ of the cross sections for two targets a and b when the distortion in the exit channel is removed, we obtain

$$R[nl,n'l'] = \frac{\sigma_a[nl,n'l']}{\sigma_b[nl,n'l']}\bigg|_{\nu_2=0} \xrightarrow[(v\to\infty)]{} \frac{I_a^2 S_a^2}{I_b^2 S_b^2}, \qquad (9)$$

where S is the slope or gradient of the HF wave function for the active electron at the origin ($x_1=0$) and, as before, I is the passive overlap integral. In Table II we present the ratios $R[1s,1s]$ for (i) $a\equiv$ He and $b\equiv H^-$ and (ii) $a\equiv Li^+$ and $b\equiv$ He. As E increases, these ratios are seen to approach the values of 52.8 for (i) and 8.86 for (ii) predicted by Eq. (9), which again illustrates how the ordering of the cross sections is dictated by the relative behavior of the target wave functions. In passing, we note that when H^-, He, and Li^+ are described by HF wave functions the passive overlap integral for $n'l'=1s$ is 0.922, 0.984, and 0.993, respectively; thus, the limiting ratios in this instance are governed essentially by the relative

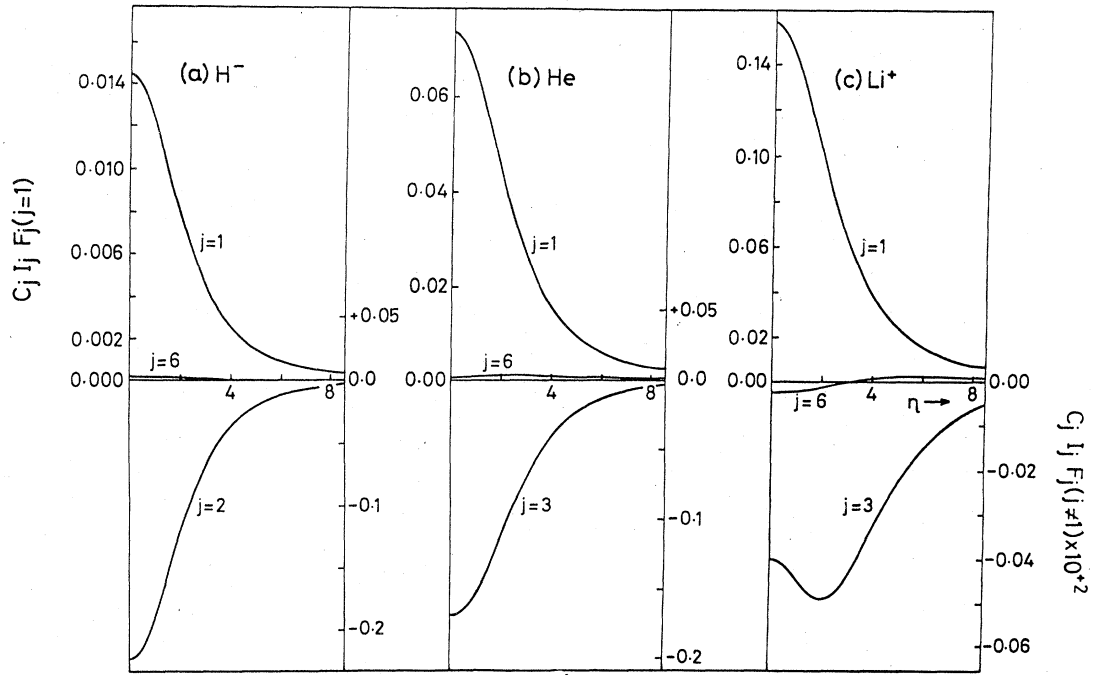

FIG. 2. Plots of $C_jI_jF_j$ vs η, defined in Eq. (10), corresponding to jth natural configuration within natural expansion formulation of $\sigma[1s,1s]_{\nu_2=0}$ for a proton impact energy of 1000 keV. (a) H^- for $j=1$, 2, and 6, (b) He for $j=1$, 3, and 6, and (c) Li^+ for $j=1$, 3, and 6. Each target was described by the natural expansion of 35-term CI wave function of Weiss,[5] and the j values quoted represent natural configurations constructed from orbitals of radial symmetry.

values of S.

If $\Phi(1,2)$ is a correlated wave function, it is of interest to examine the form of the function, say $\mathcal{F}^2$, which replaces $I^2F_1^2$ in Eq. (5). For a discussion of electron correlation, a particularly convenient form for any CI wave function is to express it as a natural expansion (see, for example, Löwdin[9]). Thus $\mathcal{F}^2$ can then be written as

$$\mathcal{F}^2 = \left[\sum_j C_j I_j \left(\sum_i b_{ij}\varphi_i(2)\,|\,n'l'\right) \times F_j\left(\eta, v, \sum_k b_{kj}\varphi_k(1), \Delta\epsilon\right)\right]^2, \tag{10}$$

where for the Weiss[5] function the basis set $\{\varphi\}$, which is used to describe $\Phi(1,2)$, consists of normalized STO's. The coefficients b_{ij} and b_{kj}, together with $\{\varphi\}$, define the natural orbitals which are given by the summations over i and k; the summation of all the natural configurations j, each weighted by the coefficient C_j, represents the total CI wave function. When $j>1$, each natural configuration in the summation corresponds to the addition of a correlation term composed of φ's with either radial or angular symmetry; when $j=1$ only, we recover the $I^2F_1^2$ term in Eq. (5). Thus, by using the natural expansion and by setting $\nu_2=0$, the nature of the influence of the correlation terms on the CDW cross section becomes transparent and we see that the *relative* importance of each natural orbital is determined solely by its occupation coefficient C_j *and* its passive overlap integral I_j. As a consequence, when improving the target wave function up to a CI description, any change in the cross section at large v will be independent of the projectile charge Z_A but may be strongly influenced by the final state of the *passive* electron. When $n'l'=1s$, I_j is nonzero only for those natural orbitals of radial symmetry; therefore, only radial correlation terms in $\Phi(1,2)$ contribute to the cross sections in the present CDW calculations. In Fig. 2 we show, for $\sigma[1s,1s]_{\nu_2=0}$, $C_jI_jF_j$ vs η for $j=1$, 3, and 6 for He and Li^+ and $j=1$, 2, and 6 for H^- at $E=1000$ keV. The curves not only indicate the dominance of the $j=1$ term but also show that as we go from H^- to Li^+ the higher natural orbitals become rapidly less important; it is noted that at $\eta=0$ for H^-, $C_2I_2F_2 \simeq \frac{1}{7}C_1I_1F_1$, while for Li^+ at $\eta=0$, $C_3I_3F_3 \simeq \frac{1}{300}C_1I_1F_1$.

III. SUMMARY

The rationalization of the trends in the present CDW cross sections became tractable by setting $\nu_2=0$. Hence we have shown that, as the projectile velocity increases, the active electron is captured from regions of increasingly higher momentum within the target atom and that in this region it is the characteristics of the wave function which govern the trends in Q when comparing different targets. The nature of the distortion acting on the captured electron in the exit channel (i.e., when $\nu_2\neq 0$) is such that it reduces the size of each cross section, and this effect will increase as Z_B increases. Thus, when considering two-electron targets of large nuclear charge, it would be interesting to see if the final distortion could ever dominate the wave function in its influence on Q and so produce trends which are the reverse of those examined here.

[1]A. Salin, J. Phys. B 3, 937 (1970).
[2]Dz. S. Belkić and R. Gayet, J. Phys. B 10, 1923 (1977).
[3]K. E. Banyard and B. J. Szuster, Phys. Rev. A 16, 129 (1977). See also J. Phys. B 10, L503 (1977).
[4]J. C. Moore and K. E. Banyard, J. Phys. B 11, 1613 (1977).
[5]A. W. Weiss, Phys. Rev. 122, 1826 (1961).
[6]E. Clementi and C. Roetti, At. Data Nucl. Data Tables 14, 177 (1974).
[7]R. F. Curl and C. A. Coulson, Proc. Phys. Soc. London 85, 647 (1964). See also J. Phys. B 1, 325 (1968).
[8]Dz. S. Belkić and R. K. Janev, J. Phys. B 6, 1020 (1973).
[9]P.-O. Löwdin, Phys. Rev. 97, 1474 (1975). See also P.-O. Löwdin and H. Shull, Phys. Rev. 101, 1730 (1956).